MERGING CLUSTER COLLABORATION: A PANCHROMATIC ATLAS OF RADIO RELIC MERGERS

N. Golovich*[1,2], W. A. Dawson[1], D. M. Wittman[2,3]
R. J. van Weeren[4,5], F. Andrade-Santos[4], M. J. Jee[2,6], B. Benson[2], F. de Gasperin[5,7], T. Venturi[8], A. Bonafede[8,9], D. Sobral[5,10], G. A. Ogrean[11,12], B. C. Lemaux[2], M. Bradač[2], M. Brüggen[7], A. Peter[13,14,15]

Submitted to ApJ: 26 June 2018

Binary Major Merger Scenario

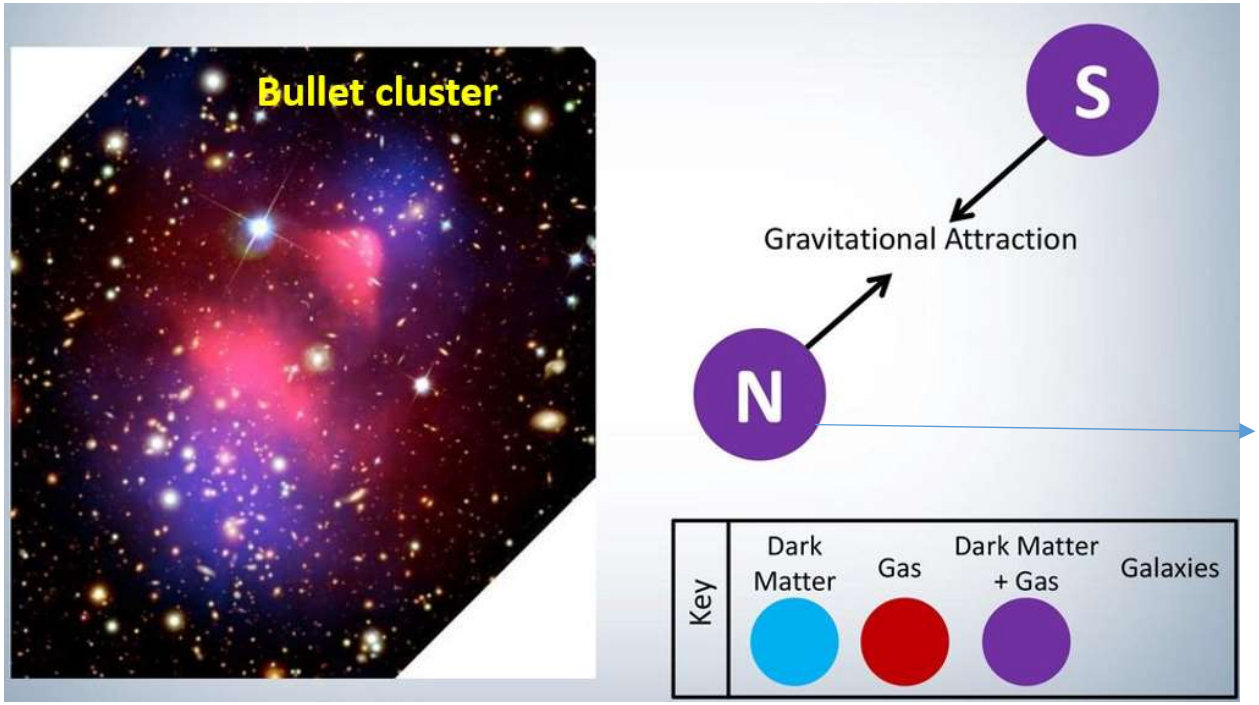

Hierarchical clustering ➔ formation of large scale structure

➔ Cluster mergers are on-going processes in the present Universe.

Subcluster composition: by mass
~85 % DM
~13 % gas
~2 % galaxies

Due to hydrodynamical forces, the gas slows down during the merger and is separated from DM.

MERGING CLUSTER COLLABORATION: A PANCHROMATIC ATLAS OF RADIO RELIC MERGERS

N. Golovich*[1,2], W. A. Dawson[1], D. M. Wittman[2,3]
R. J. van Weeren[4,5], F. Andrade-Santos[4], M. J. Jee[2,6], B. Benson[2], F. de Gasperin[5,7], T. Venturi[8], A. Bonafede[8,9], D. Sobral[5,10], G. A. Ogrean[11,12], B. C. Lemaux[2], M. Bradač[2], M. Brüggen[7], A. Peter[13,14,15]

Submitted to ApJ: 26 June 2018

Bullet Cluster Merger: https://youtu.be/rLx_TXhTXbs

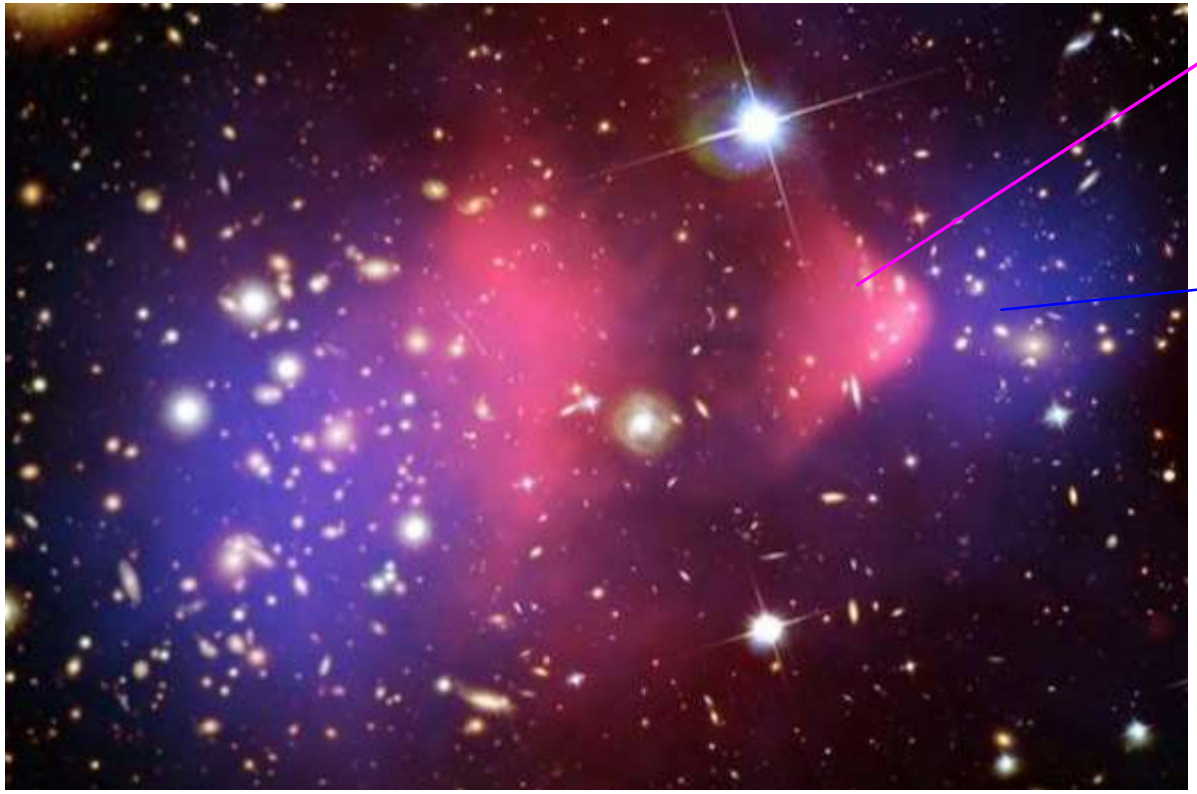

X-ray from hot ICM gas

Matter (galaxy + DM) distribution inferred from gravitational weak lensing.

Separation between the gas and non-collisional matter.
➔ Impling Existence of DM

Due to hydrodynamical forces, the **hot X-ray gas (shown in pink)** slows down during the merger and is separated from **the galaxies & DM**. The **total mass distribution (shown in blue)** inferred from gravitational lensing, is coincident with the position of the galaxies.

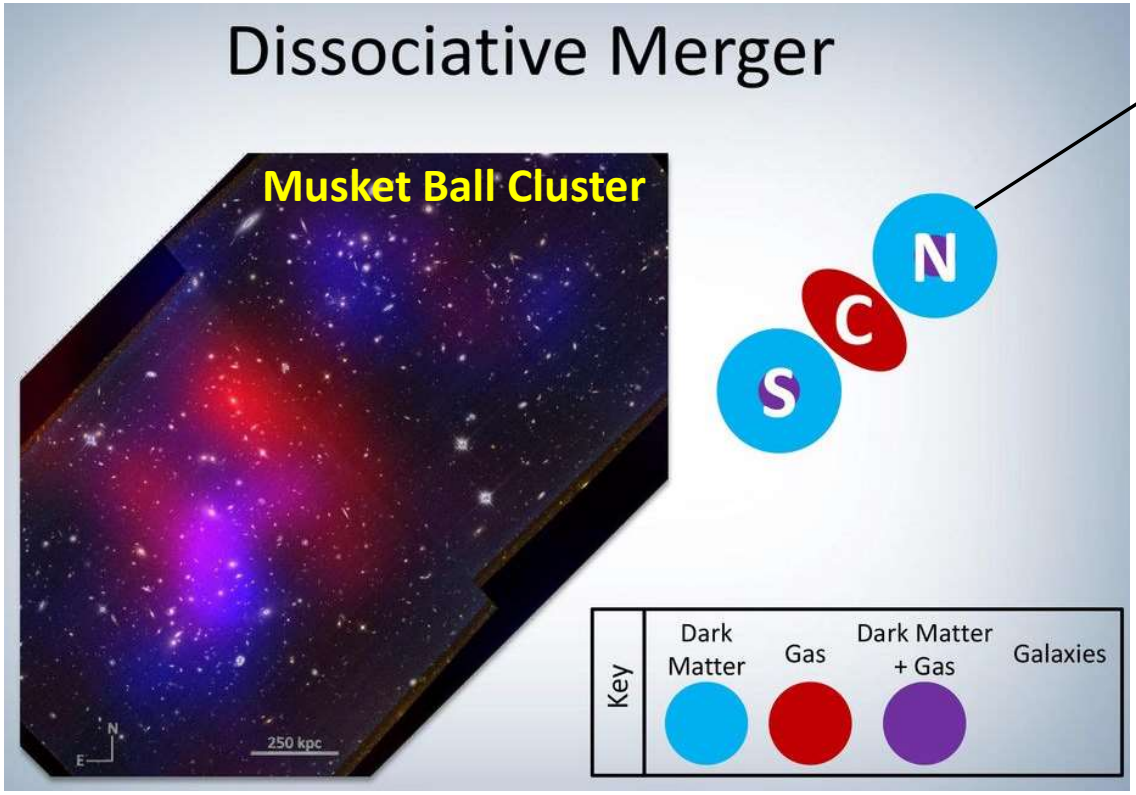

-**Gas** & **DM** offset

As the subclusters approach and pass through pericenter the gas halos exchange momentum, while the galaxies and DM continue well past pericenter.

➔A **separation** arises between **the gas** and the outbound **galaxies and DM**

➔ dissociative mergers

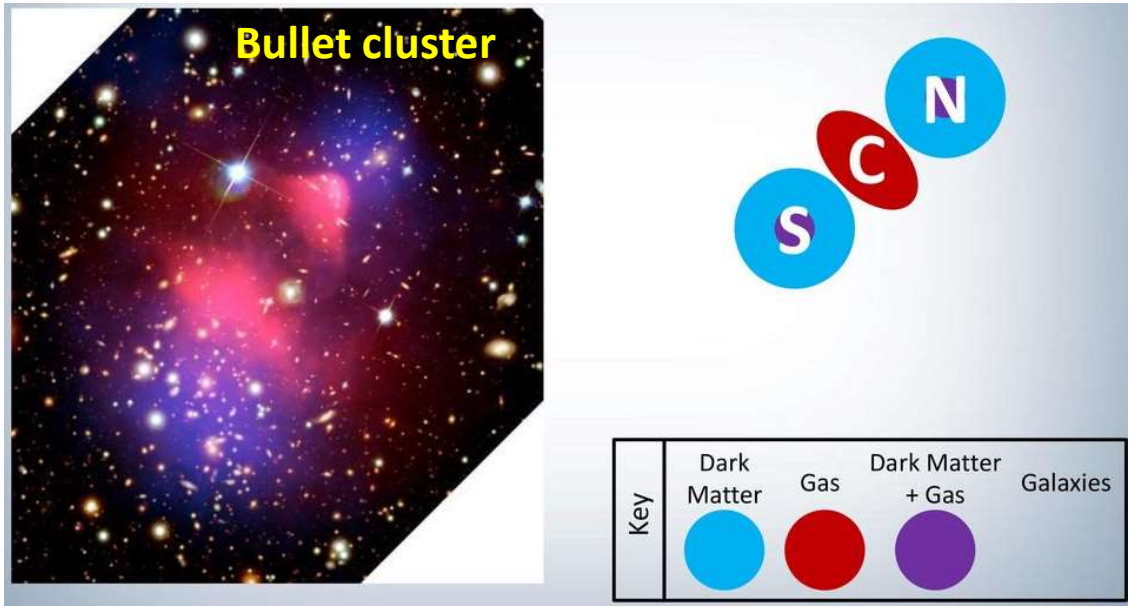

Subcluster composition:
by mass
~85 % DM
~13 % gas
~2 % galaxies

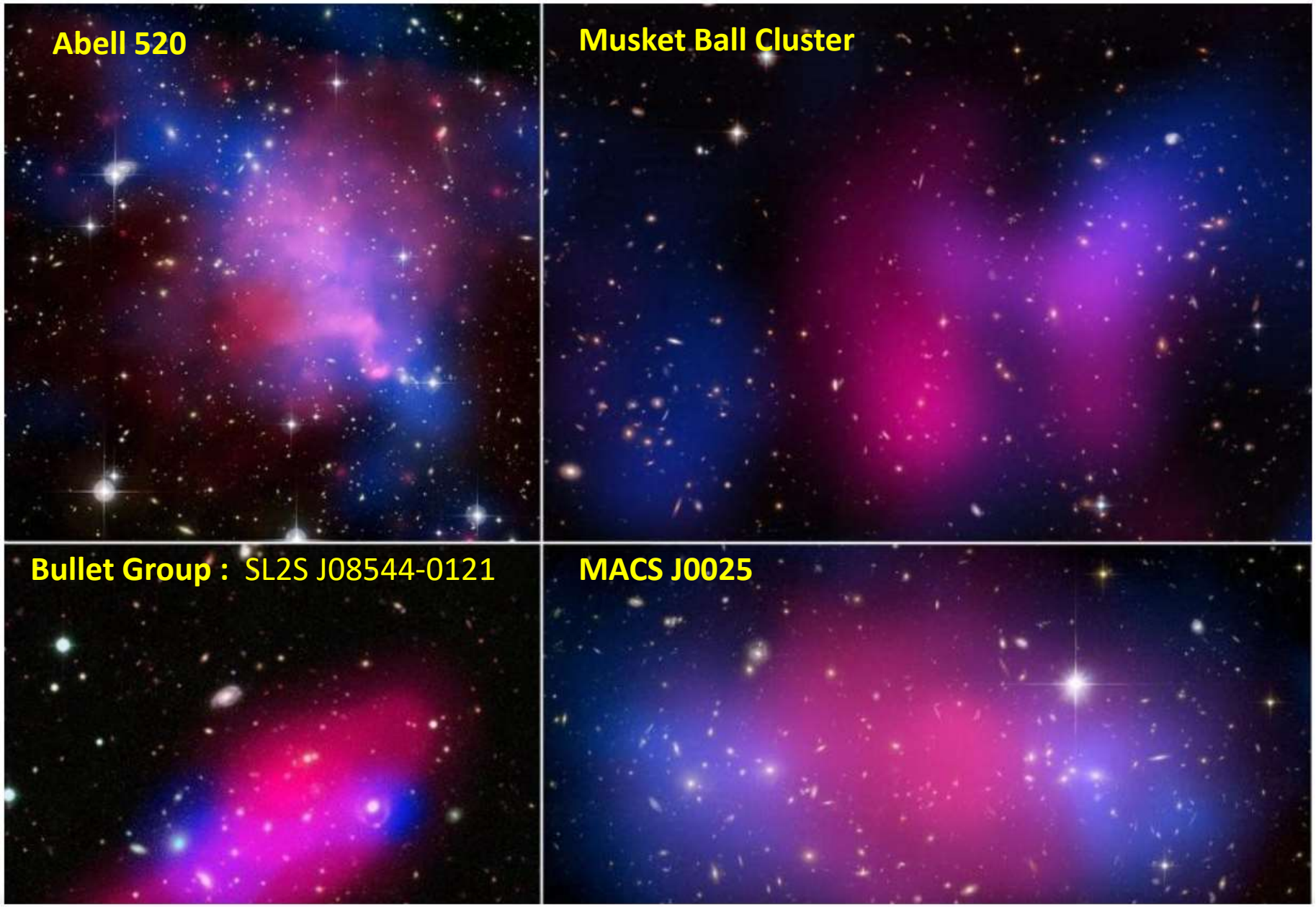

Dissociative merging clusters showing the separation between **X-rays (pink)** and **gravitational mass (blue).**

The speed of the 'bullet' in the merging galaxy cluster 1E0657−56

Volker Springel[1]★ and Glennys R. Farrar[2]

SPH+N-body simulation

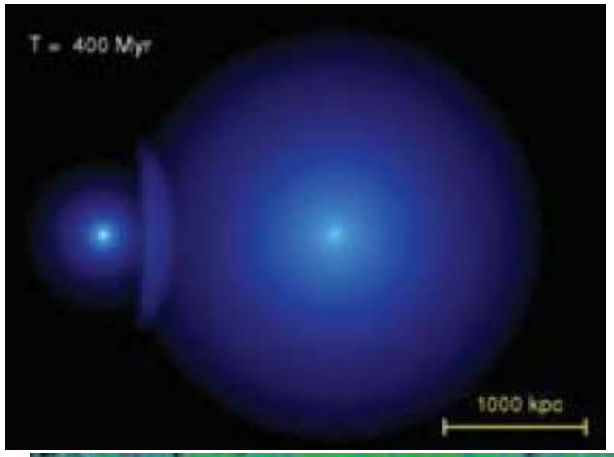

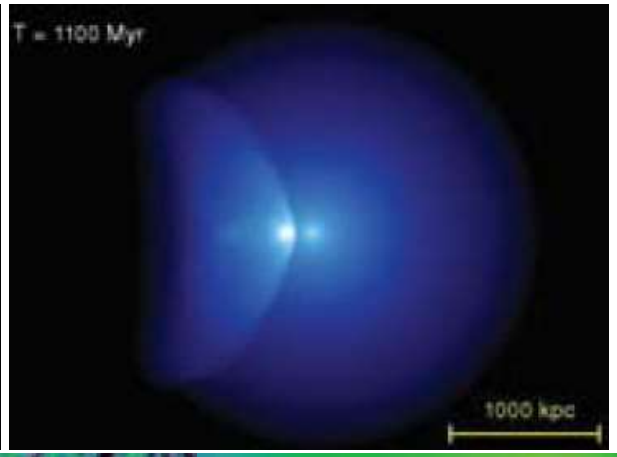

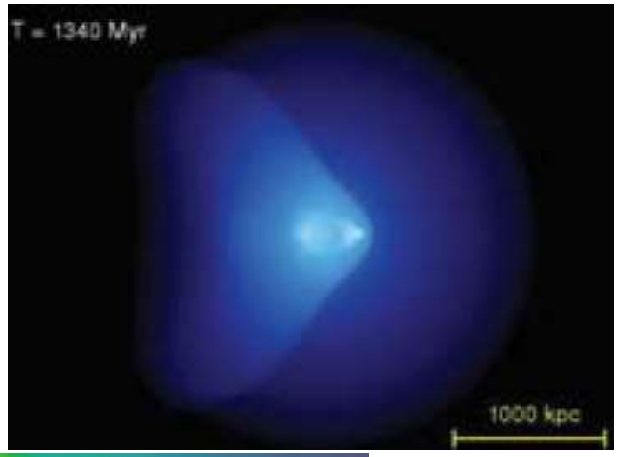

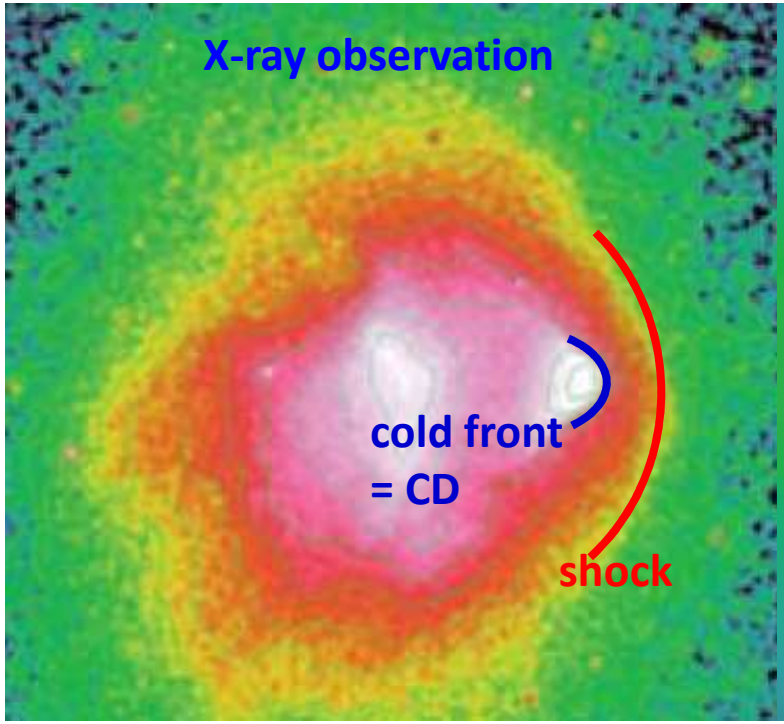

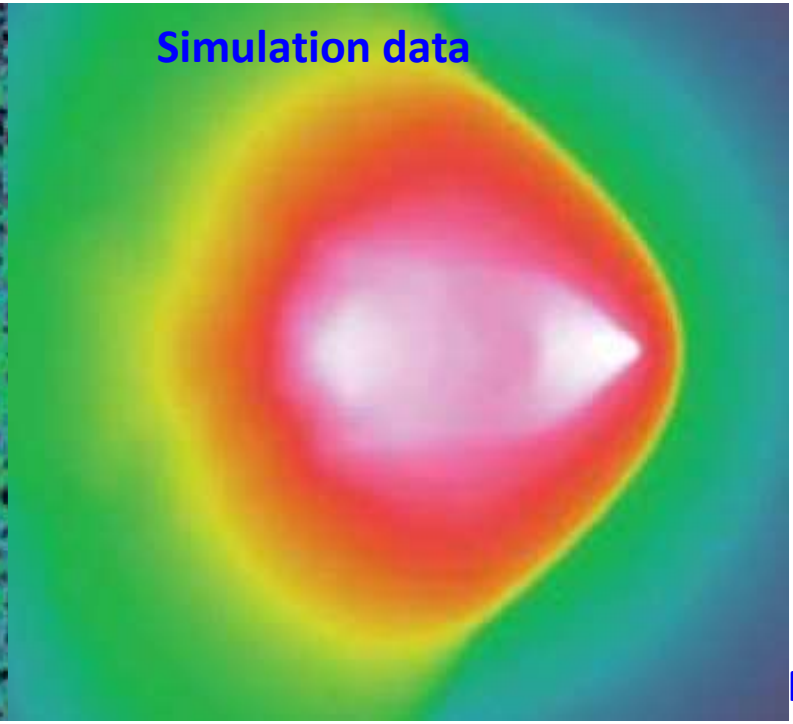

MNRAS 2007

MERGING CLUSTER COLLABORATION: A PANCHROMATIC ATLAS OF RADIO RELIC MERGERS

N. Golovich[*1,2], W. A. Dawson[1], D. M. Wittman[2,3]
R. J. van Weeren[4,5], F. Andrade-Santos[4], M. J. Jee[2,6], B. Benson[2], F. de Gasperin[5,7], T. Venturi[8], A. Bonafede[8,9], D. Sobral[5,10], G. A. Ogrean[11,12], B. C. Lemaux[2], M. Bradač[2], M. Brüggen[7], A. Peter[13,14,15]

Submitted to ApJ: 26 June 2018

Observation of 29 merging clusters with radio relics:

- Optical photometry+ spectroscopy ➔ mapping of mass and galaxy distribution

- X-ray ➔ mapping of hot ICM gas

- Radio ➔ relativistic electrons accelerated by ICM shocks

Modeling of merger dynamics:

- Dynamics modeling of mergers: N-body cosmological simulations

- HD or MHD simulations

- Weak lensing for matter distribution

- DM self-interaction model

- Particle acceleration at shocks

Detection of radio relics means that the merger axis is likely to lie in the plane of sky with small line-of-sight velocities (galaxies)

➔ selection condition: viewed edge-on

http://www.mergingclustercollaboration.org/

Lawrence Livermore Nat'l Lab

Will Dawson

- Weak lensing, spectroscopy, X-ray
- Dynamics modeling of mergers
- Importance sampling to match simulations with observations

UC Davis

Marusa Bradac

- Weak + strong lensing

Nathan Golovich

- Spectroscopy
- Dynamic modeling

James Jee

- Weak lensing: shape measurement and mass reconstruction

Karen Ng

- Weak lensing
- Extension to dynamical modeling
- Implementation of analysis pipeline for both data and simulations

David Wittman

- Weak lensing

UC Irvine

James Bullock

- Self-interacting dark matter theory
- Simulation theory
- Simulation analysis

Oliver Elbert

- Merging simulations

Manoj Kaplinghat

- Self-interacting dark matter theory

Miguel Rocha

- Code implementation of algorithms
- Production of simulations
- Analysis and visualization of simulation data

Ohio State University

Annika Peter

- Self-interacting dark matter theory
- Simulation analysis

Stacy Kim

- Self-interacting dark matter simultions

Lisbon Observatory

David Sobral

- Galaxy evolution

Oxford

Julian Merten

- Weak + strong lensing
- Analysis of simulation data
- Comparison between simulations and observations data and its interpretation

Hamburg

Marcus Bruggen

- Hydrodynamics merging cluster simulations
- Radio relic simulation/theory
- High-energy astrophysics

Harvard-Smithsonian CfA

Reinout van Weeren

- Radio relic observation and analysis
- HIgh-energy astrophysics and intra-cluster medium physics

ESO Garching

Andra Stroe

- Galaxy evolution

San Franscisco State

Andisheh Mahdavi

- X-ray analysis
- Joint cluster mass estimation

Subjects

- Weak lensing (DM)
- dynamics modeling
- simulations
- radio relics
- spectroscopy
- self-interactions of DM
- galaxy evolution
- X-ray analysis

Weak lensing by Galaxy Clusters ➔ DM distribution

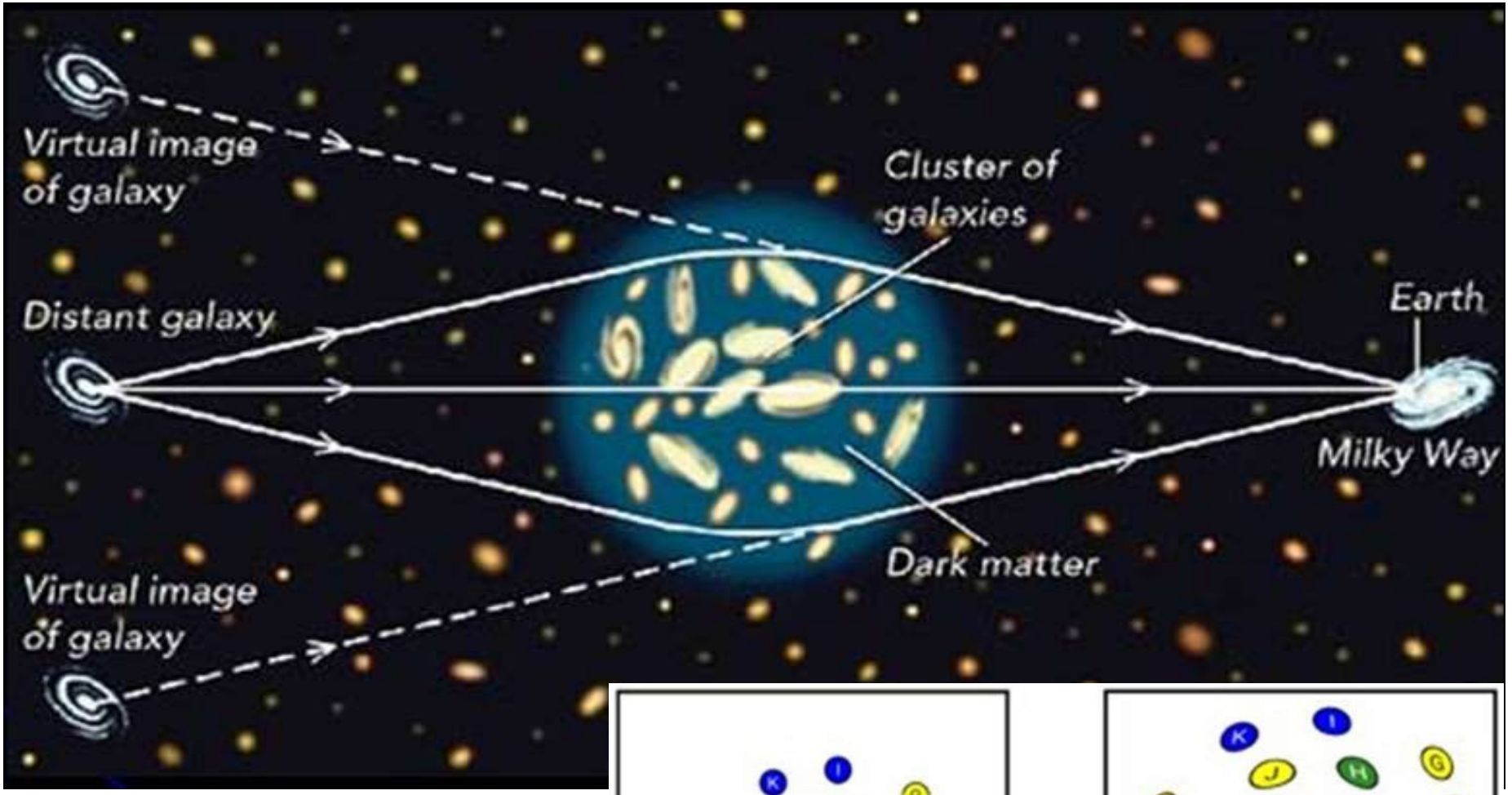

Rings, arclets, distorted & magnified images due to gravitational lensing by foreground clusters.

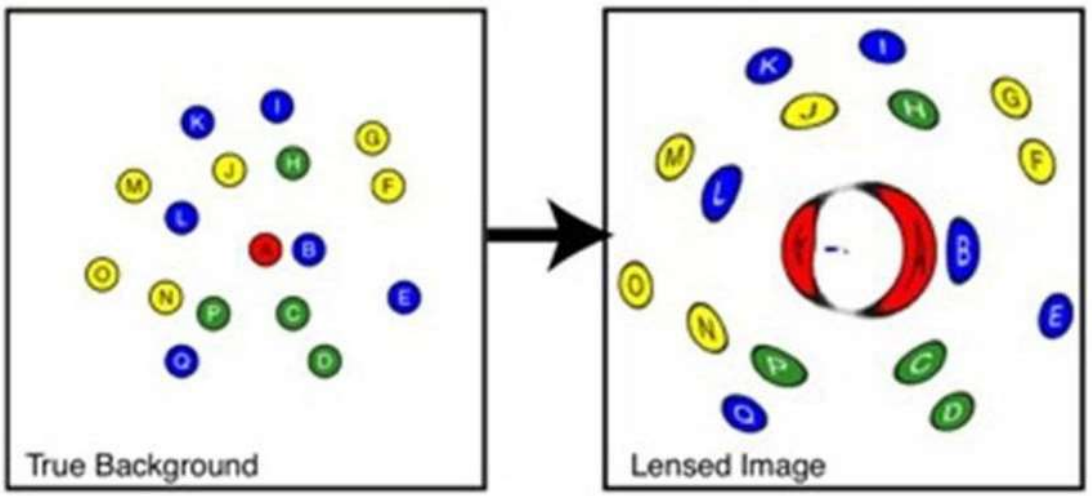

MC^2: MAPPING THE DARK MATTER DISTRIBUTION OF THE "TOOTHBRUSH" CLUSTER RX J0603.3+4214 WITH *HUBBLE SPACE TELESCOPE* AND SUBARU WEAK LENSING*

M. James Jee[1,2], William A. Dawson[3], Andra Stroe[4], David Wittman[2], Reinout J. van Weeren[5], Marcus Brüggen[6], Maruša Bradač[2], and Huub Röttgering[4]

ApJ 2016

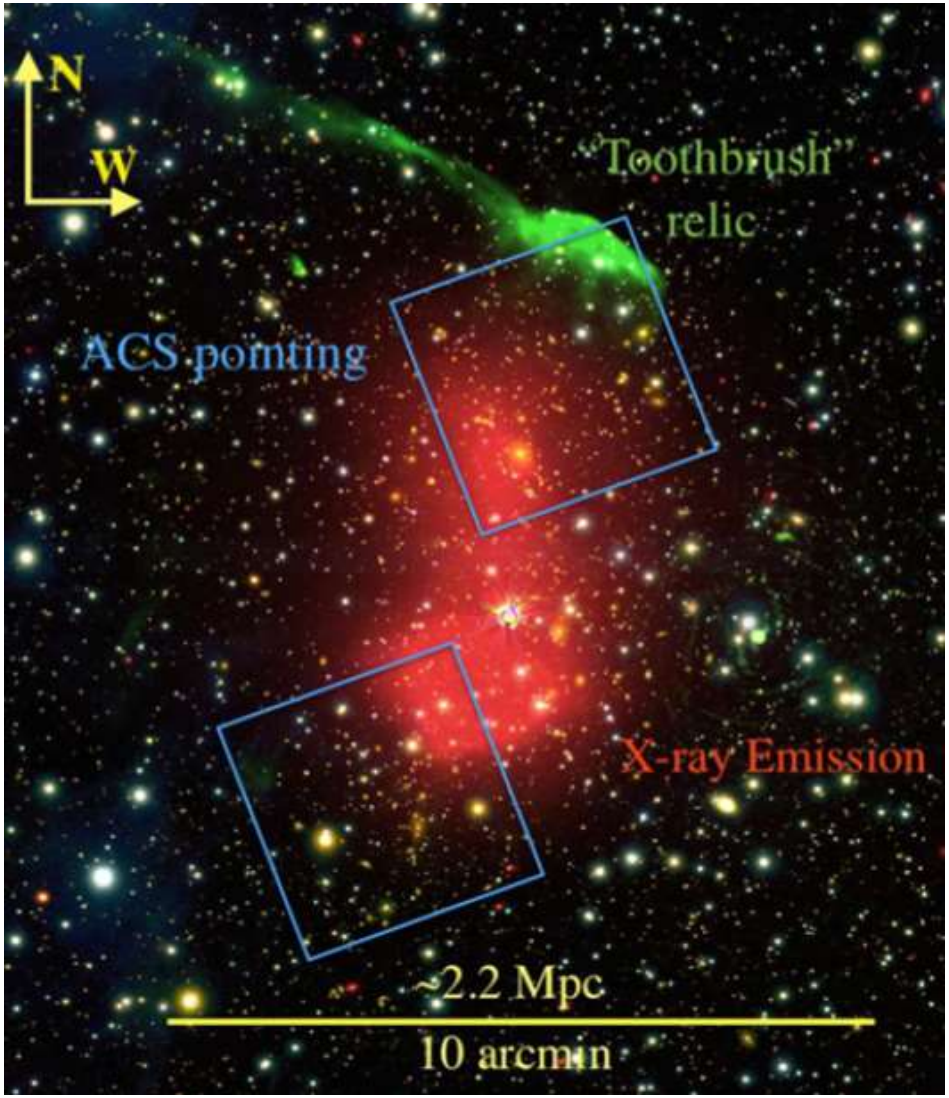

offset between X-ray and mass peaks

mass reconstruction (contours) from optical image

cartoon picture for binary major merger ➔ merger driven shocks

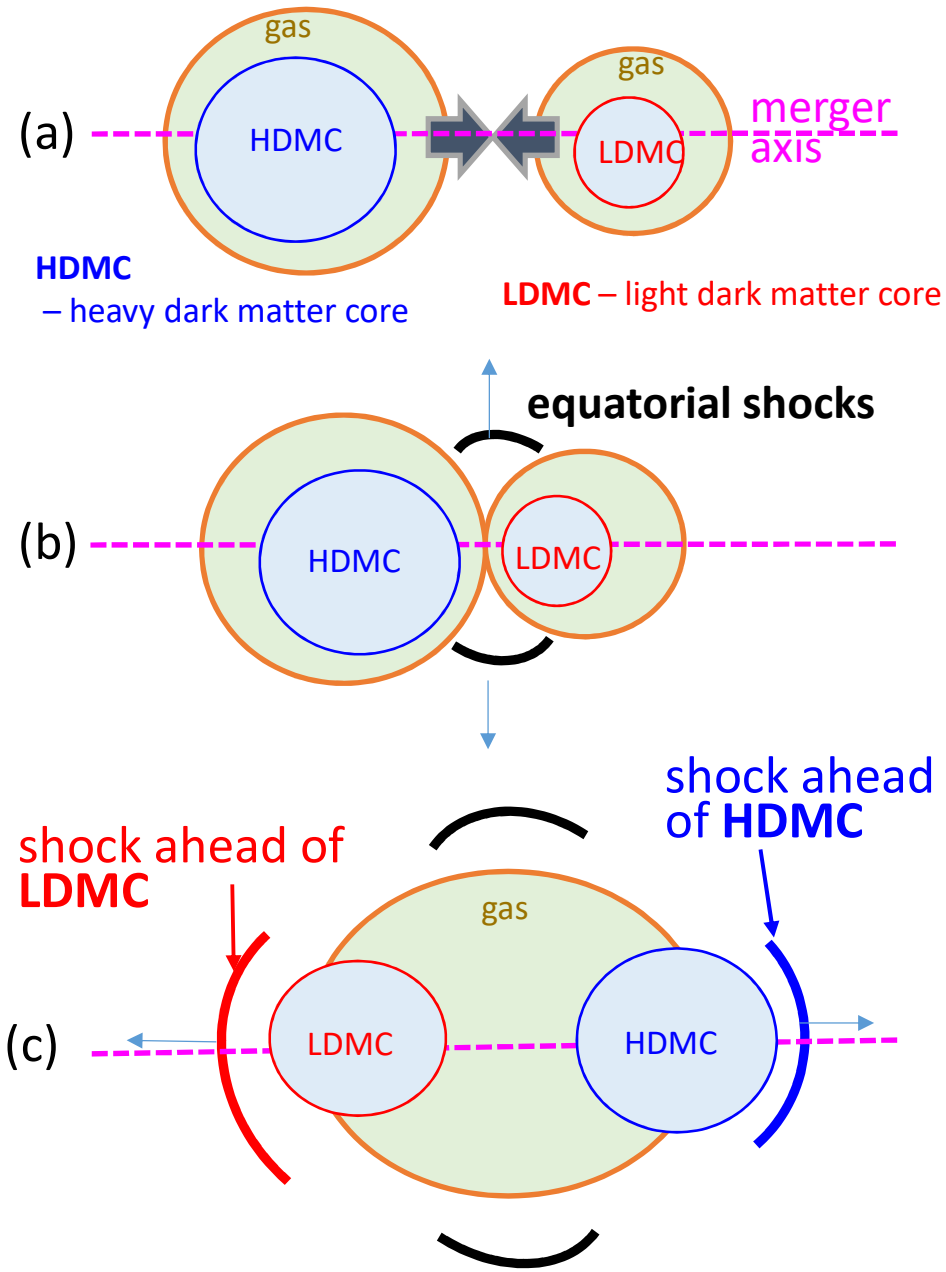

Two subclumps are approaching.

'Equatorial Shocks' are launched first perp. to the merger axis.

DM core passage (pericenter)

Two 'axial shocks' form and propagate along the merger axis.

➔ acceleration of electrons via DSA

➔ Synchrotron emission

➔ form double radio relics

EVOLUTION OF SHOCKS AND TURBULENCE IN MAJOR CLUSTER MERGERS

S. PAUL[1,4], L. IAPICHINO[2], F. MINIATI[3], J. BAGCHI[4], AND K. MANNHEIM[1] ApJ 2011

color: Temperature, contours: gas density

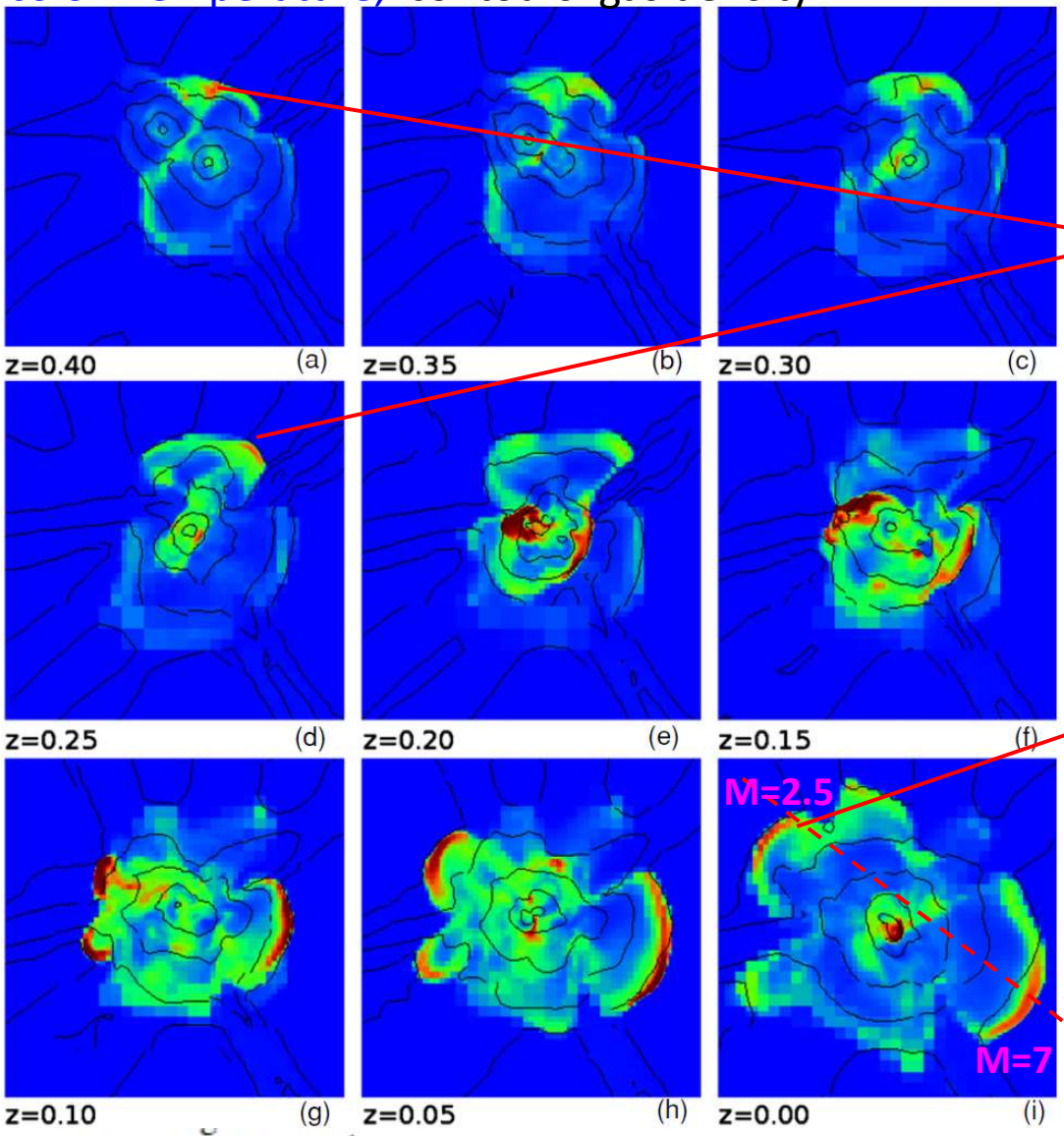

Overview of the Performed Simulations

Run	Redshift of the Merger	M_1 ($10^{13}\,M_\odot$)	M_2 ($10^{13}\,M_\odot$)	Δ_m	M_f ($10^{14}\,M_\odot$)
F	0.3	7.23	4.23	0.59	2.62

mass ratio

Equatorial shock

Set of cosmological simulations: Enzo code.

The simulation box has a comoving size of 128 Mpc h^{-1}

Merger shocks

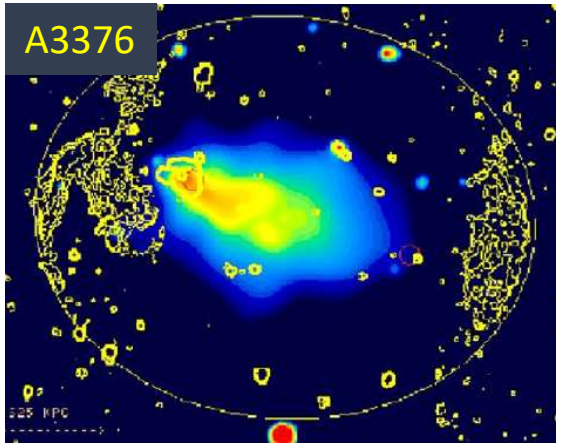

Properties of merger shocks in simulated merging clusters

Ha, Ryu, & Kang 2018

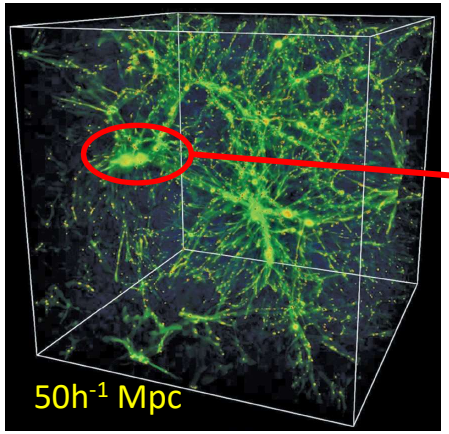

Identify merging clusters

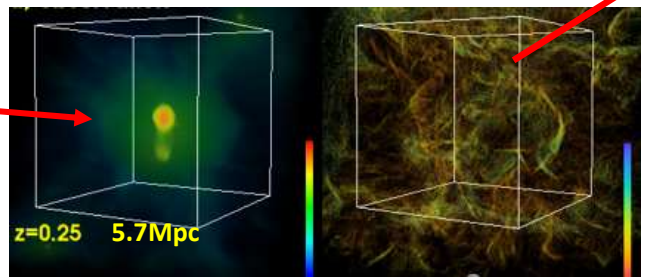

X-ray emissivity

Shock Mach number

Find three types of shocks associated with each merging cluster.

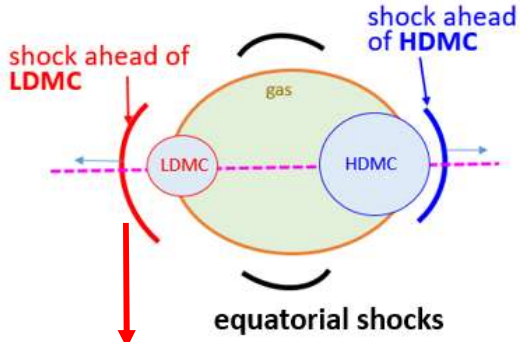

CR electron acceleration via DSA➔ radio relic

1. Performed several LCDM cosmological simulations with 1024^3 grids on 50 h^{-1} Mpc box
2. Identify merging clusters going through almost head-on collision with ~ 2:1 mass ratio & kT_x ~ 5 KeV

Main Results

- Shocks driven by major mergers have Mach number M_s ~ 2 – 4 at 1-2 Mpc from the cluster center at ~1 Gyr after DM core passage.
- Properties of merger shocks are consistent with observations of radio relics detected in the outskirts of galaxy clusters.
- DSA at merger shocks can reproduce most of the radio observations of radio relics.

(double) Radio relics: diffuse radio sources found mainly in merging clusters

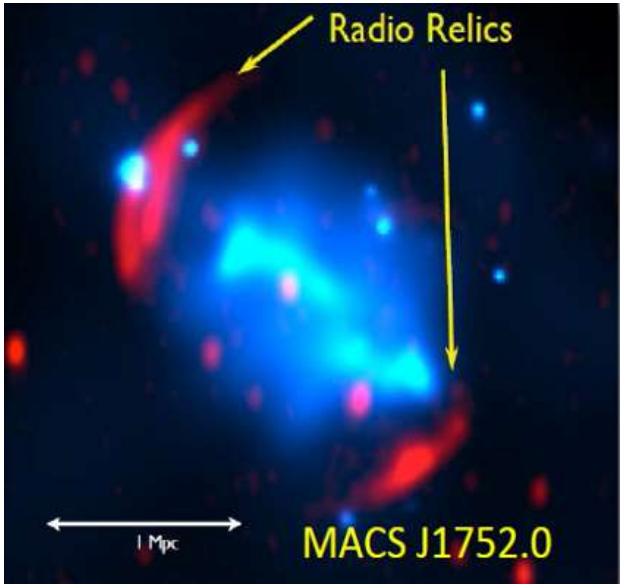

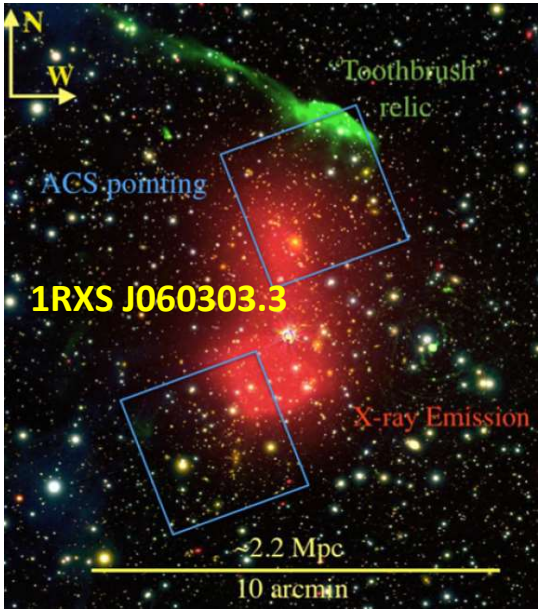

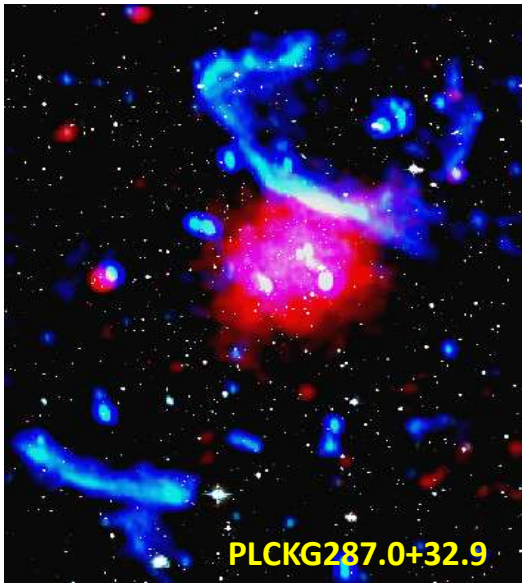

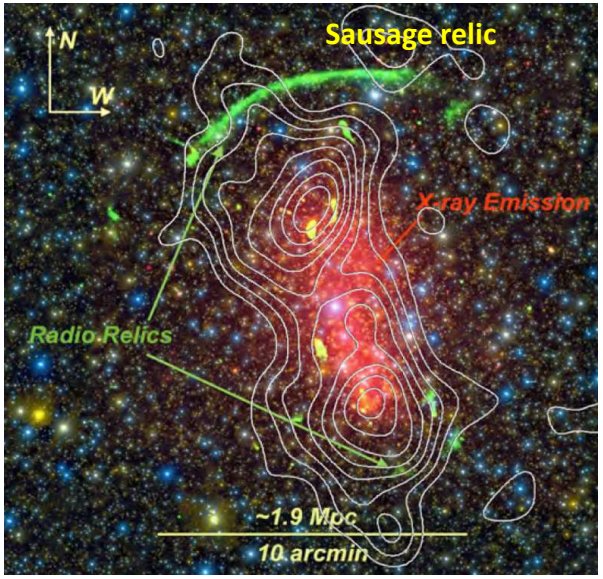

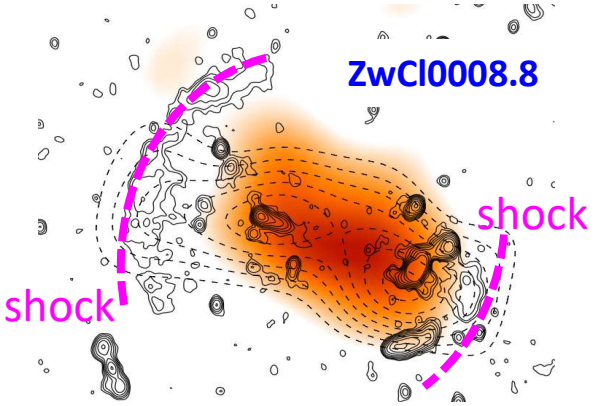

$$M^2_{\text{radio}} = \frac{(3+2\alpha_{\text{sh}})}{(2\alpha_{\text{sh}}-1)}$$

$$\Rightarrow M_{\text{radio}}$$

α_{sh} : radio spectral index

Radio relics: synchrotron emission from relativistic electrons accelerated by merger-driven shocks.
Shock Mach numbers can be estimated from the spectral index, based on DSA model.

Synchrotron emission from a single electron

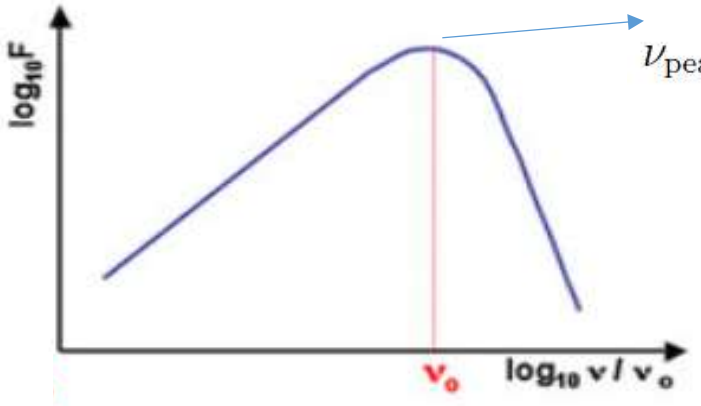

$$\nu_{\rm peak} \approx 0.3(\frac{3eB}{4\pi m_e c})\gamma_e^2 \approx 0.63\ {\rm GHz}\cdot(\frac{B}{5\ \mu{\rm G}})(\frac{\gamma_e}{10^4})^2$$

Electron energy spectrum due to DSA

$$f_e(r_s, p) \propto p^{-q} \quad \text{at the shock}$$

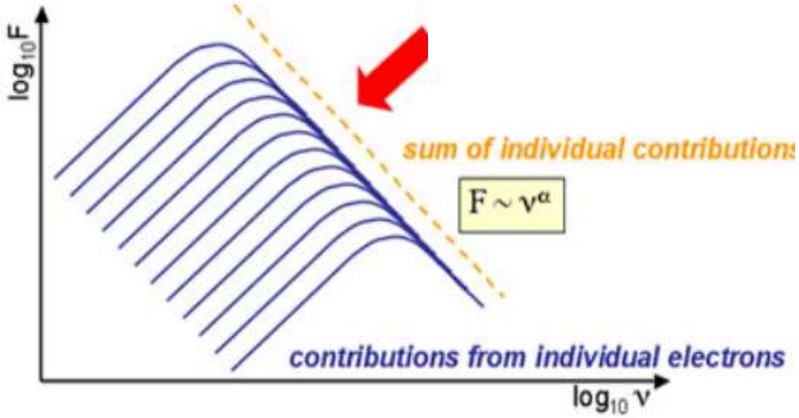

Synchrotron radiation spectrum

$$j_\nu(r_s) \propto \nu^{-\alpha_{\rm shock}} \quad \text{at the shock}$$

$$\alpha_{\rm shock} = (q-3)/2 = (M^2+3)/2(M^2-1)$$

$$t_{\rm rad}(\gamma_e) = \frac{p}{b(p)} = 9.8\times10^7\ {\rm yr}\left(\frac{B_{\rm e}}{5\ \mu{\rm G}}\right)^{-2}\left(\frac{\gamma_e}{10^4}\right)^{-1}$$

synchrotron/iC cooling behind the shock

➔ Steepening of f(p) ➔ steepening of j_ν

$$B_{e,2} = \sqrt{B_2^2 + B_{\rm rad}^2}$$

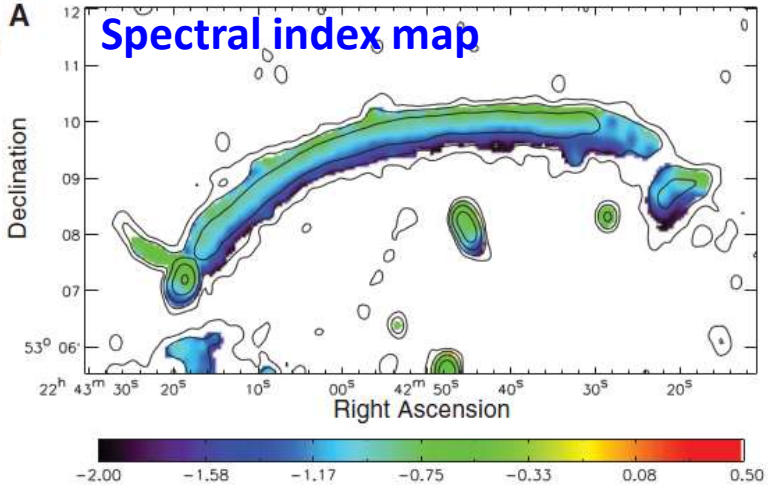

Sausage Relic

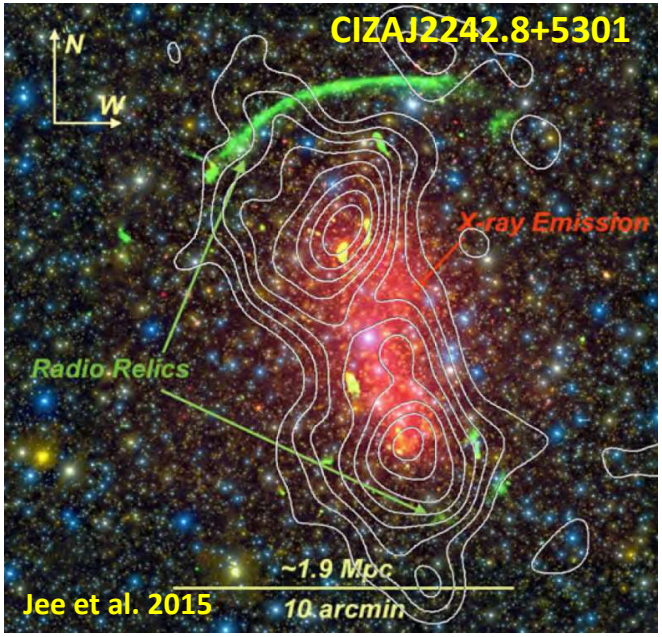

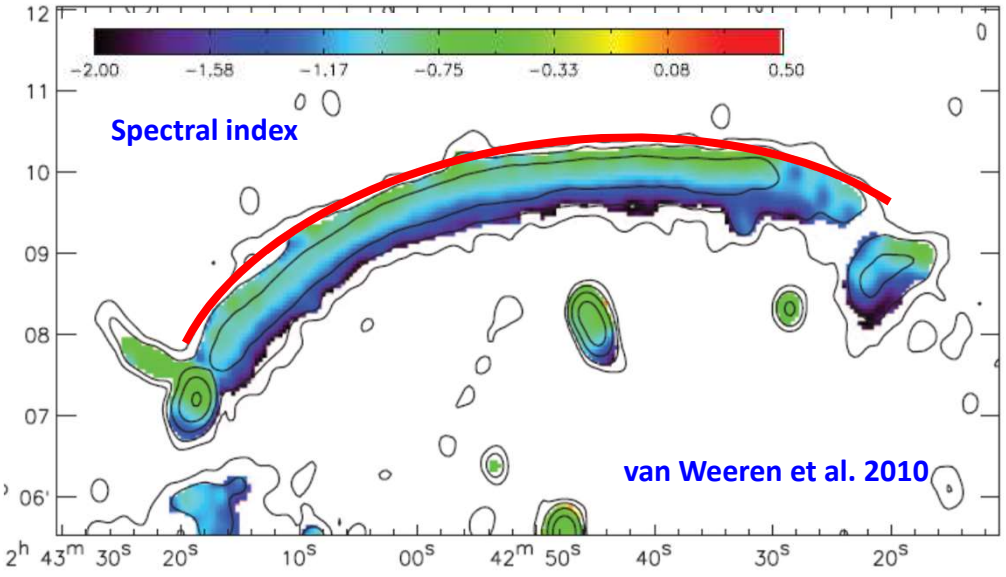

$$M_{\text{radio}} \approx 2.7$$

(Hoang + 2017)

$$\frac{T_2}{T_1} = \frac{(M_X^2+3)(5M_X^2-1)}{16M_X^2}$$

$$\Rightarrow M_X \approx 2.7$$

(Akamatsu + 2015)

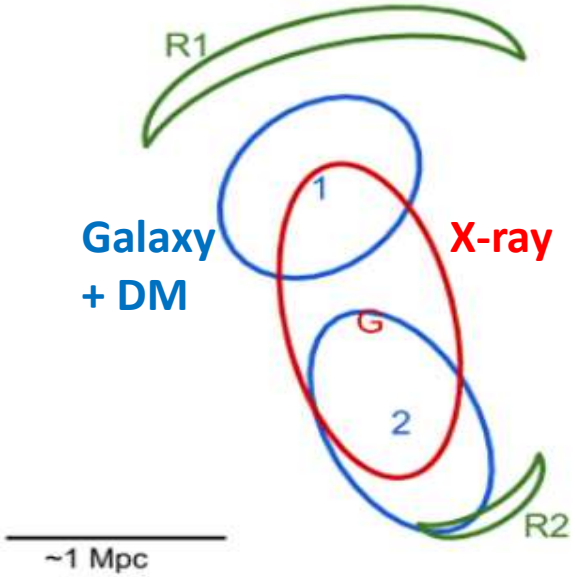

double radio relics (RN + RS) could be direct evidence for merger-driven shocks !

http://www.mergingclustercollaboration.org/

Signatures of shocks in ICM: X-ray shocks in merging clusters

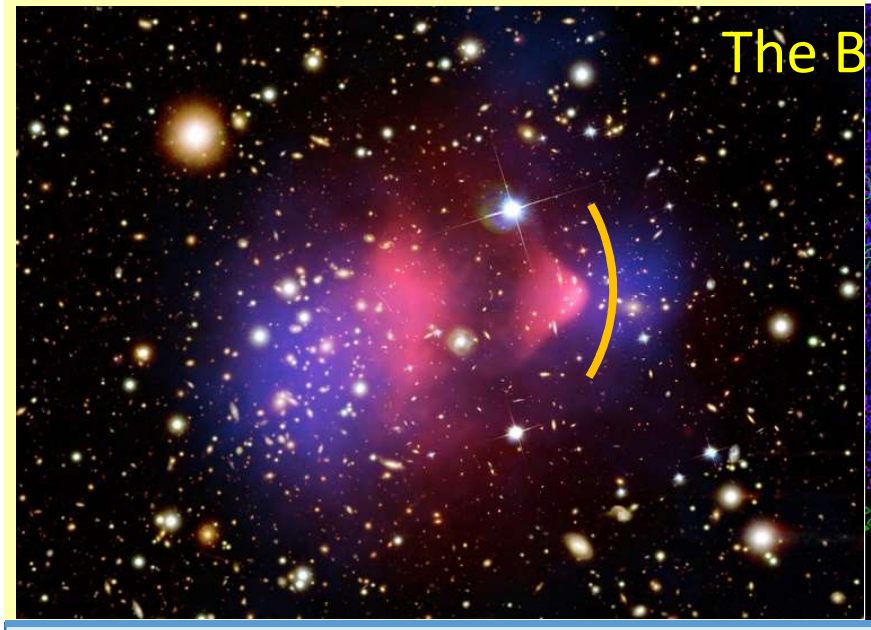

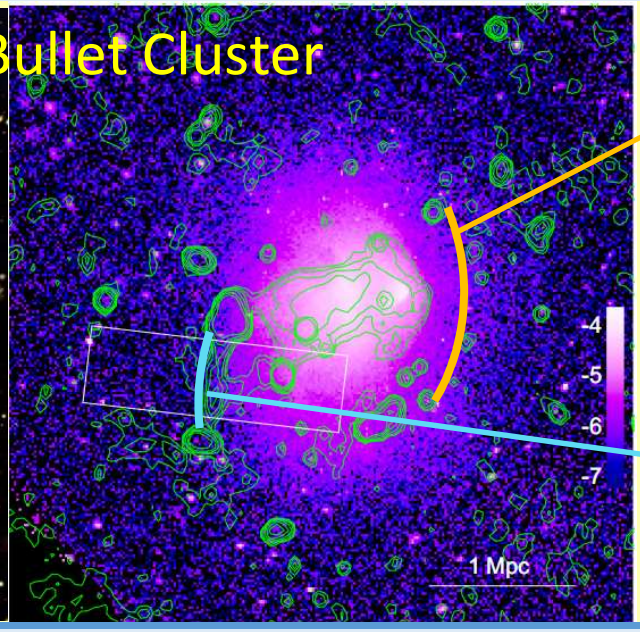

$M_X \approx 3.0$

Markevitch 2006

$M_X \approx 2.5$

Shimwell et al. 2015

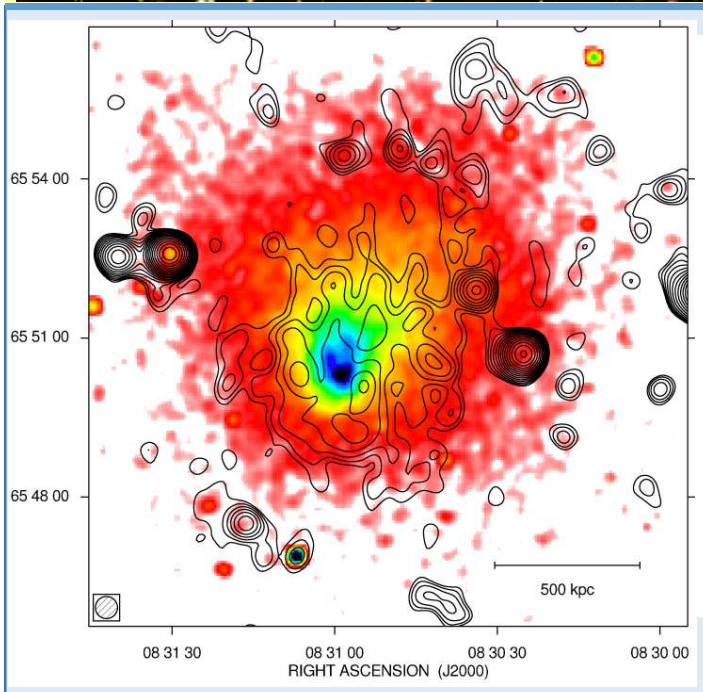

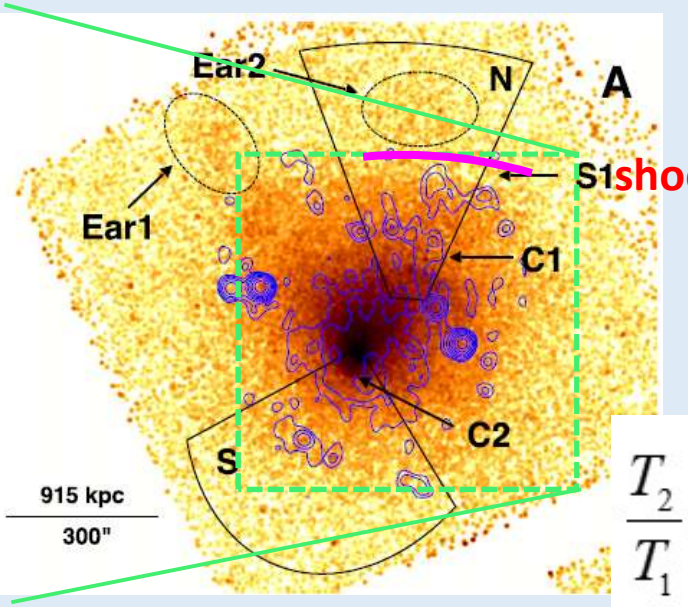

Cluster A665

$M_X = 3 \pm 0.6$

Dasadia et al. 2016

$$\frac{T_2}{T_1} = \frac{(M_X^2 + 3)(5M_X^2 - 1)}{16 M_X^2}$$

Cluster 1RXS J060303.3 with the Toothbrush radio relic

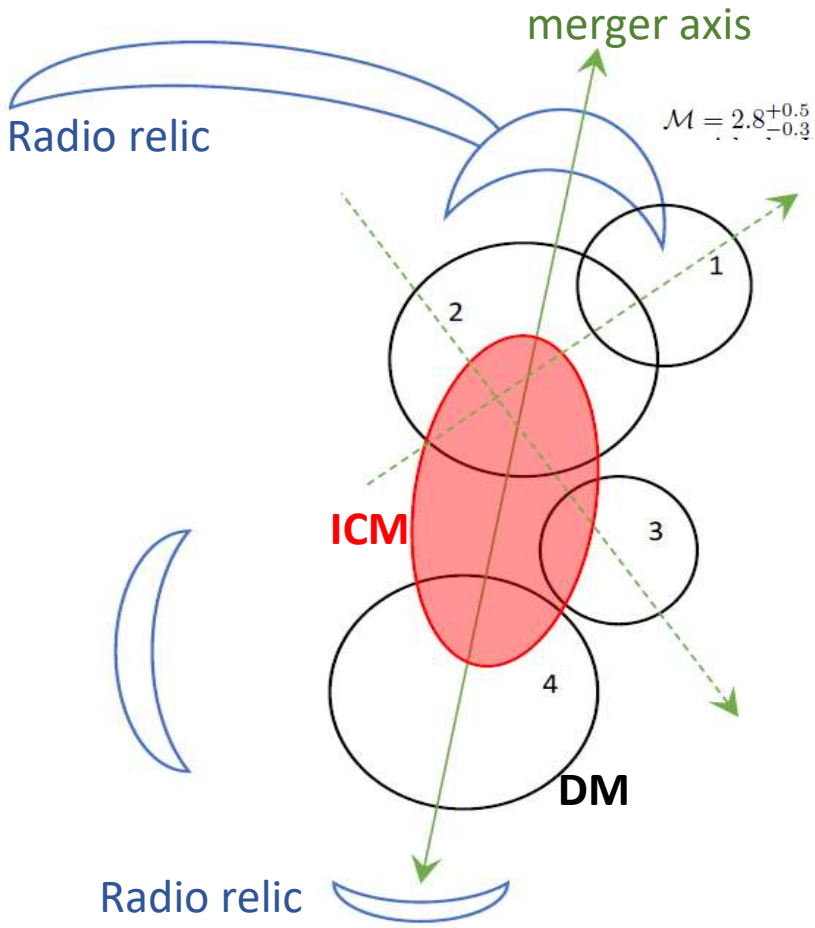

Gaussian mixture model (**GMM**) analysis
➔ Identity subclusters

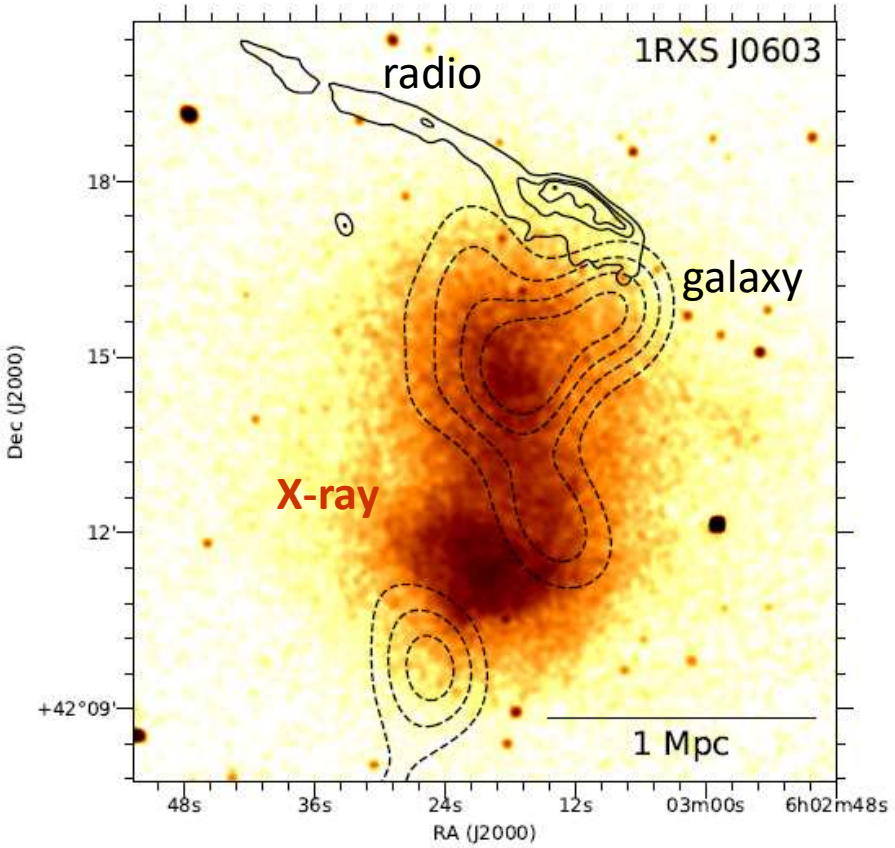

offset between X-ray and mass peaks

Table 1
The Merging Cluster Collaboration radio-selected sample.

29 merging clusters with radio relics

Cluster	Short name	RA	DEC	Redshi
1RXS J0603.3+4212	1RXSJ0603	06:03:13.4	+42:12:31	0.226
Abell 115	A115	00:55:59.5	+26:19:14	0.193
Abell 521	A521	04:54:08.6	-10:14:39	0.247
Abell 523	A523	04:59:01.0	+08:46:30	0.104
Abell 746	A746	09:09:37.0	+51:32:48	0.214
Abell 781	A781	09:20:23.2	+30:26:15	0.297
Abell 1240	A1240	11:23:31.9	+43:06:29	0.195
Abell 1300	A1300	11:32:00.7	-19:53:34	0.306
Abell 1612	A1612	12:47:43.2	-02:47:32	0.182
Abell 2034	A2034	15:10:10.8	+33:30:22	0.114
Abell 2061	A2061	15:21:20.6	+30:40:15	0.078
Abell 2163	A2163	16:15:34.1	-06:07:26	0.201
Abell 2255	A2255	17:12:50.0	+64:03:11	0.080
Abell 2345	A2345	21:27:09.8	-12:09:59	0.179
Abell 2443	A2443	22:26:02.6	+17:22:41	0.110
Abell 2744	A2744	00:14:18.9	-30:23:22	0.306
Abell 3365	A3365	05:48:12.0	-21:56:06	0.093
Abell 3411	A3411	08:41:54.7	-17:29:05	0.163
CIZA J2242.8+5301	CIZAJ2242	22:42:51.0	+53:01:24	0.189
MACS J1149.5+2223	MACSJ1149	11:49:35.8	+22:23:55	0.544
MACS J1752.0+4440	MACSJ1752	17:52:01.6	+44:40:46	0.365
PLCKESZ G287.0+32.9	PLCKG287	11:50:49.2	-28:04:37	0.383
PSZ1 G108.18-11.53	PSZ1G108	23:22:29.7	+48:46:30	0.335
RXC J1053.7+5452	RXCJ1053	10:53:44.4	+54:52:21	0.072
RXC J1314.4-2515	RXCJ1314	13:14:23.7	-25:15:21	0.247
ZwCl 0008.8+5215	ZwCl0008	00:08:25.6	+52:31:41	0.104
ZwCl 1447+2619	ZwCl1447	14:49:28.2	+26:07:57	0.376
ZwCl 1856.8+6616	ZwCl1856	18:56:41.3	+66:21:56.0	0.304
ZwCl 2341+0000	ZwCl2341	23:43:39.7	+00:16:39	0.270

Toothbrush

Sausage Relic

Simple, bimodal systems with double relics

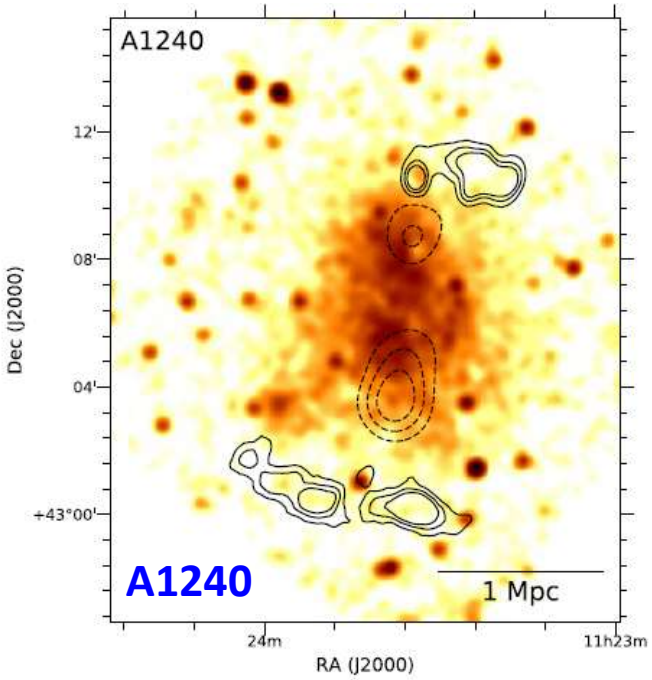

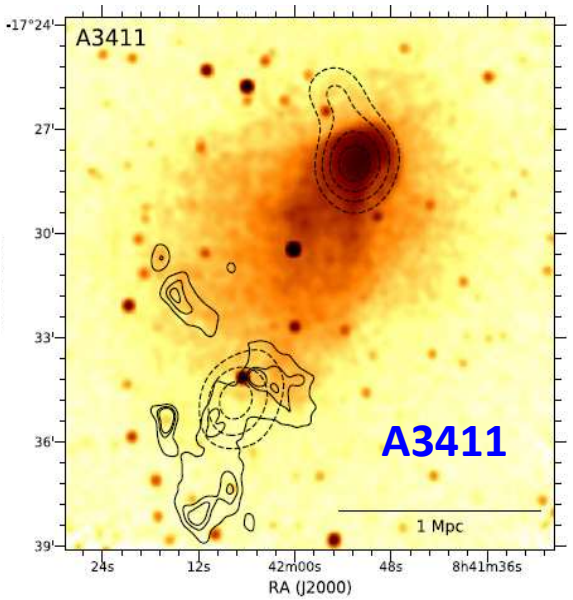

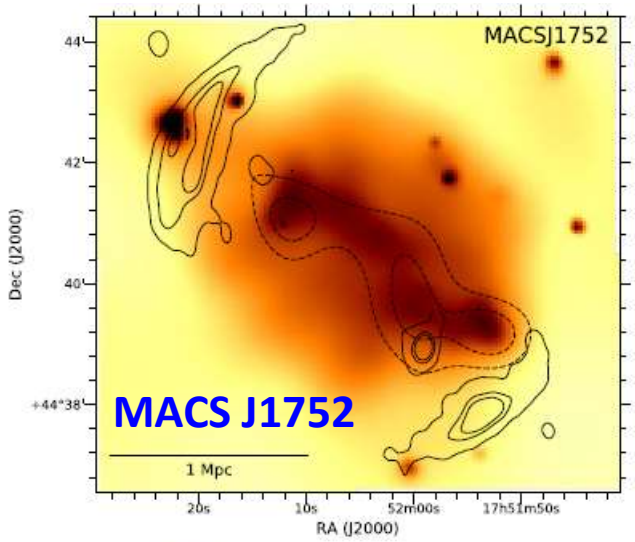

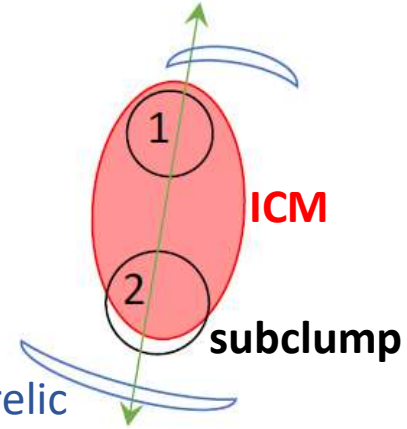

ICM

subclump

Radio relic

merger axis

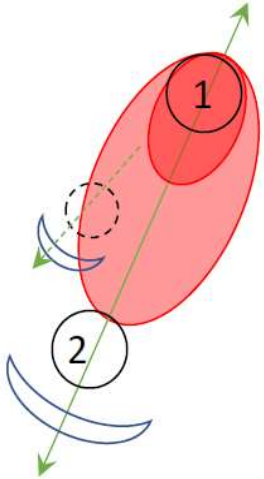

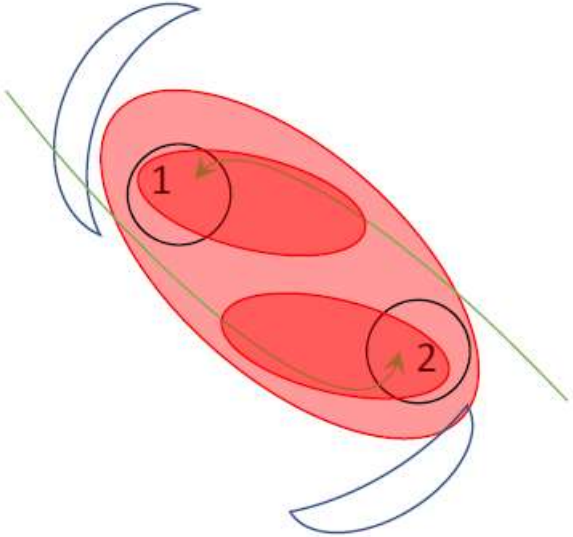

Simple, bimodal systems with double relics

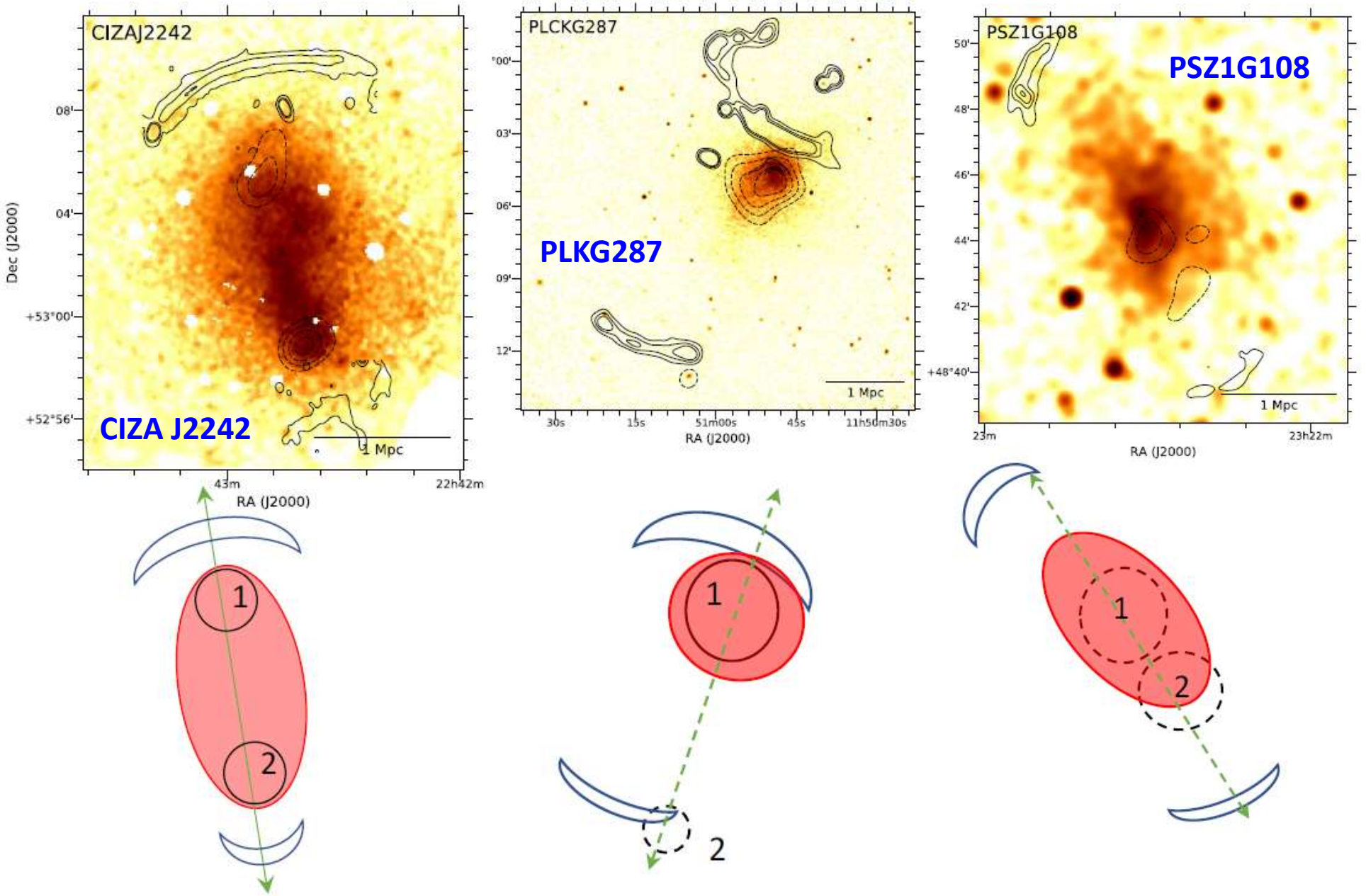

Simple, bimodal systems with double relics

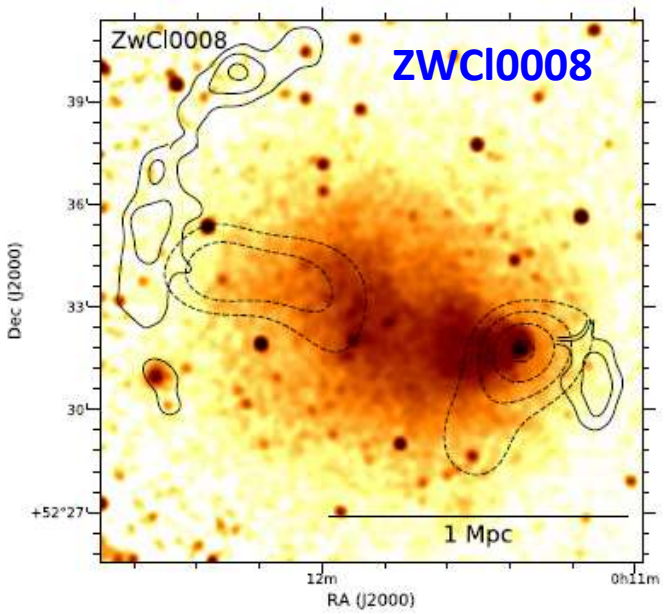

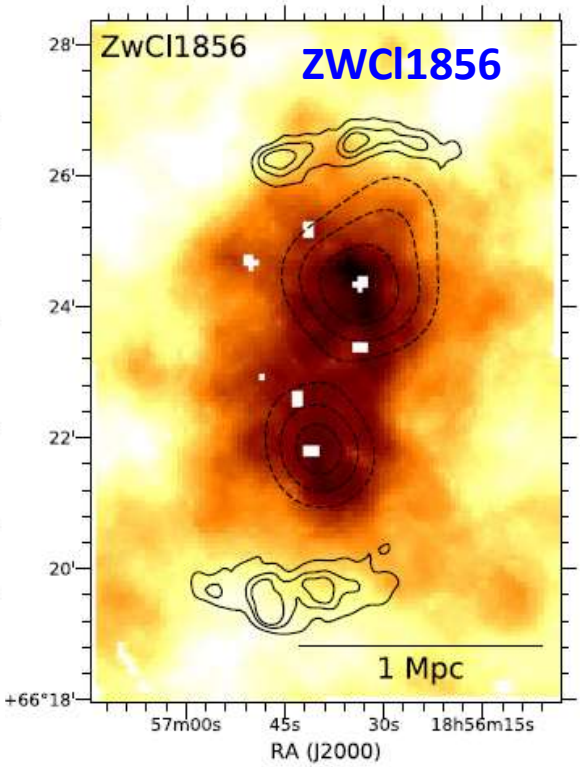

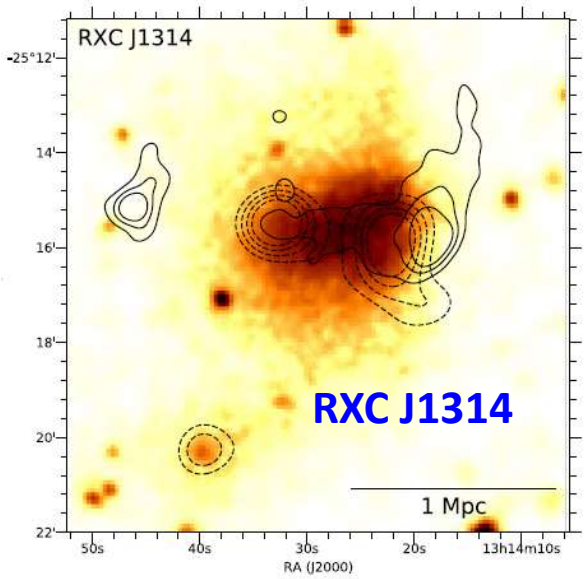

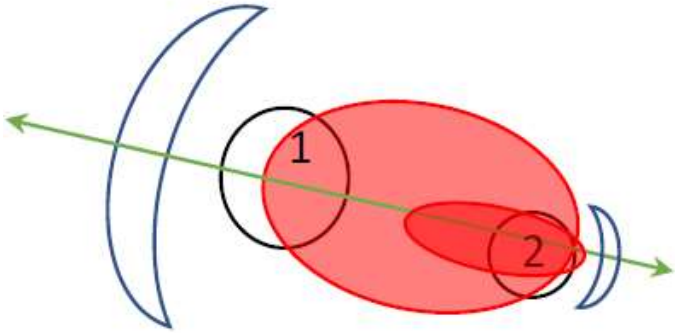

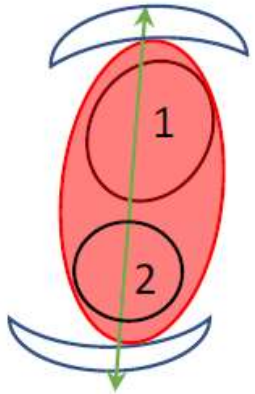

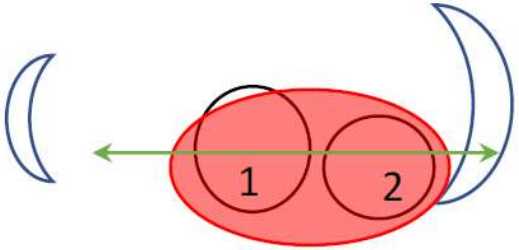

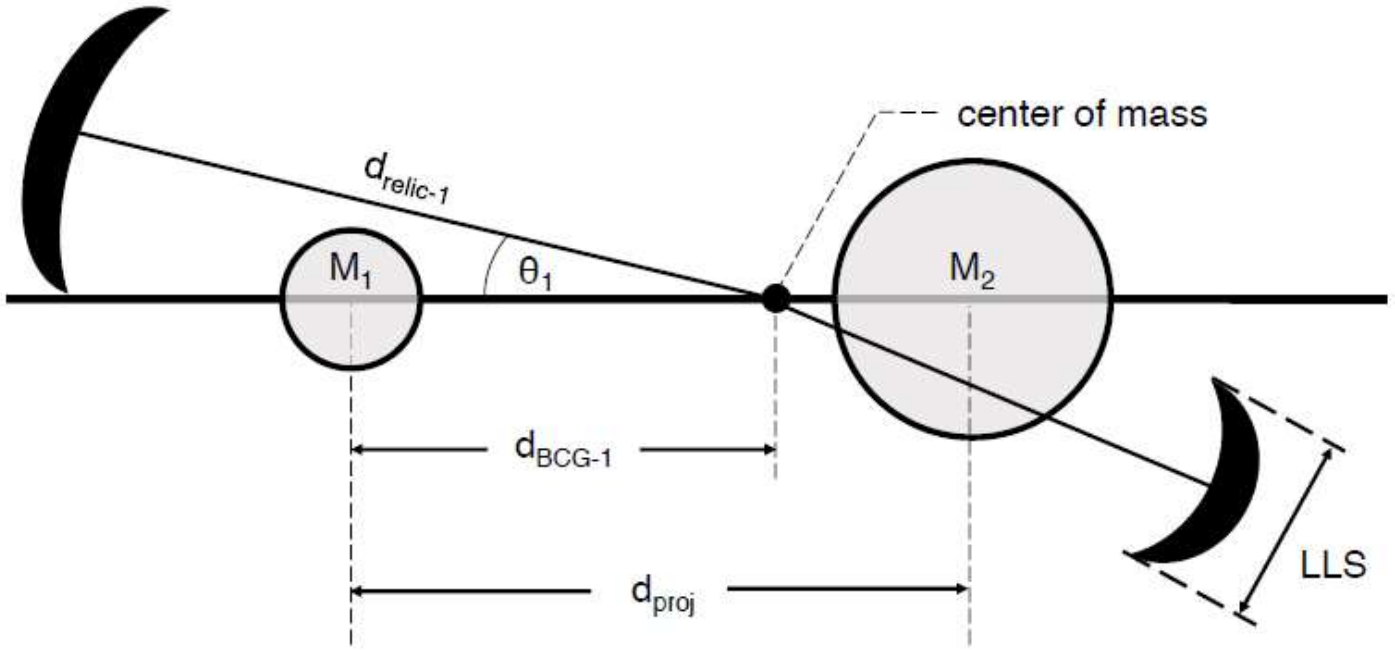

Schematic representation of the relic geometry for a double relic system (e.g. A1240).

-The line of sight velocity difference between merging subclusters is small.
- Radio relics are a robust indicator of the merger axis: merger activity aligned with the radio relic.
- Double radio relics are a strong indicator of simple merger geometries.

Mergers with double radio relics means that the merger axis is likely to lie in the plane of sky with small line-of-sight velocities (galaxies)
➔ viewed edge-on